J Solid State Electrochem (2006) 10: 894–904
DOI 10.1007/s10008-005-0014-x

ORIGINAL PAPER

A. Arancibia · J. Henriquez-Roman · M. A. Páez
L. Padilla-Campos · J. H. Zagal · J. Costamagna
G. Cárdenas-Jirón

# Influence of 5-chloro and 5-methyl benzotriazole on the corrosion of copper in acid solution: an experimental and a theoretical approach

Received: 24 February 2005 / Revised: 7 April 2005 / Accepted: 12 May 2005 / Published online: 30 July 2005


**Abstract** The inhibition of copper corrosion in aerated 0.1 mol $l^{-1}$ hydrochloric acid solutions was studied using electrochemical polarization in the presence of different concentrations of benzotriazole and its two derivatives, 5-chloro and 5-methyl benzotriazole. The inhibition efficiencies obtained from cathodic Tafel plots increased markedly with increase in the additive concentration. Benzotriazole and 5-methyl-benzotriazole were found to be cathodic type corrosion inhibitors for concentrations higher than $10^{-4}$ mol $l^{-1}$ . However, the 5-chloro-benzotriazole was found to be a mixed inhibitor for concentrations up to $10^{-3}$ mol $l^{-1}$, above this concentration the inhibitor behaves as an anodic type inhibitor. The inhibitors are physisorbed on the copper surface following a Langmuir's isotherm. The inhibition efficiencies depended on the inhibitor concentration and follows the order 5-chloro-benzotriazole > 5-methyl-benzotriazole > 1-H-benzotriazole. From the theoretical calculations, the change in the inhibition mechanism observed for 5-chloro-benzotriazole at concentrations higher than $10^{-3}$ mol $l^{-1}$ is associated with the electronic acceptor characteristic of chloro, which increases the benzotriazole acidity allowing the formation of CuBTA.

**Keywords** Copper corrosion · Benzotriazole · Theoretical calculations

A. Arancibia · J. Henriquez-Roman · M. A. Páez (✉)
J. H. Zagal · J. Costamagna · G. Cárdenas-Jirón
Departamento de Química de los Materiales,
Facultad de Química y Biología,
Universidad de Santiago de Chile,
40, Correo 33, Casilla, Santiago, Chile
E-mail: mpaez@lauca.usach.cl

L. Padilla-Campos
Departamento de Química, Facultad de Ciencias Básicas,
Universidad de Antofagasta, Casilla 170, Antofagasta, Chile

## Introduction

1,2,3-Benzotriazole is one of the most effective and widely used organic compounds for corrosion inhibition of copper [1–11]. From the early works of Cotton et al. [1, 2] and Poling [3], the inhibiting action of this additive has been associated with its chemisorption on the copper substrate and the formation of a polymeric coating involving Cu–benzotriazole complexes $(Cu–BTA)_n$. The effect of pH and the preexistence of cuprous oxide on the formation of the polymeric film is still a matter of debate. Thus, the polymer film thickness in chloride solutions is reported to be thinner at high pH than at low pH [4], while in sulphate solutions the polymer has been found to grow at high pH [5, 6]. On the other hand, Cu–BTA is reported to grow on $Cu_2O$ interfaces in solutions containing chloride, with a pH dependent growth linked to the stability of $Cu_2O$ [7–10], however, a CuCl interlayer preceding Cu–BTA formation has also been suggested [11]. From thermodynamic considerations and *E*–pH diagrams, it has been proposed that at high pH adsorption of BTAH onto the oxide-free copper surface, $(Cu–BTAH)_{ads}$, come first to the formation of CuBTA in the diffusion layer, which forms a polymeric film as it adsorbs onto the initial $(Cu–BTAH)_{ads}$ [12, 13]. At low pH however, the inability to form $Cu(BTA)_n$, reduces the effectiveness of benzotriazole [13].

Several workers have investigated derivatives of BTAH [14–17] and have suggested that the inhibition efficiency (IE) of benzotriazole can be improved by the introduction of proper substituents [14–20]. Regarding the mechanism of chemisorption of organic compounds on metal surfaces, it has been commonly recognized that organic inhibitors usually promote formation of a chelate on the metal surface, which includes the transfer of electrons from the organic compounds to metal, forming coordinate covalent bonds [21]. In this way the metal acts as an electrophile, whereas the nucleophilic centers of the inhibitor molecule are normally hetero atoms with

free electron pairs, which are readily available for sharing to form a bond. Considering this, the effect of substituents in related molecules, e.g. anilines, aliphatic amines, amides, benzotriazoles on the inhibitive efficiencies, have been correlated with a number of molecular properties, such as orbital energies, dipole moments, charge densities, heats of formation and ionization potentials [22–26]. In most of this work, the effect of substituents in the inhibiting efficiency has been related to the difference of the inhibitor's $E_{LUMO}$ and the metal surface's $E_{HOMO}$. However, there is some controversy in the literature concerning this point and some authors have suggested that there is no direct correlation between the efficiency of the inhibitor compounds and individual molecular parameters [27].

The aim of this work is to investigate the influence of an electron acceptor (-chloro) and an electron donor (-methyl) groups on the protective characteristic of benzotriazole in 0.1 mol $l^{-1}$ HCl. In addition, the dependence of the corrosion current density on the inhibitor concentration and of the corrosion potential on the Hammett parameter are also considered. Finally, the influence of substituent on the inhibiting efficiency of benzotriazole is analyzed with regards to theoretical calculations carried out to study the effect of substituent on the acidic characteristic of benzotriazole.

## Experimental details

### Electrochemical experiments

A polycrystalline Cu (99.999%) electrode was used for electrochemical experiments. Prior to each electrochemical measurement, the working electrode was polished with emery paper (800 and 1,200 grit size) and rinsed with ethanol in an ultrasound bath. The measurements were performed in 0.1 mol $l^{-1}$ HCl without and with the addition of different concentrations of the inhibitors.

The experimental arrangement consisted of a standard three-electrode cell, Cu-working electrode, Pt-counter electrode and a $Hg/Hg_2SO_4$ reference electrode. The measurements were performed at room temperature, after the open circuit potential (OCP) was stabilized to 3 mV per 5 min. The potentiodynamic measurements were carried out with a microprocessor controlled potentiostat (AUTOLAB). The potential was scanned 200 mV in both anodic and cathodic directions, starting from the corresponding OCP. The potential scan rate was 0.1 mV $s^{-1}$.

The inhibition efficiency (IE, %) was calculated using the corrosion current density values in the absence and presence of the inhibitor, applying the following relation:

$$IE = \left(\frac{i^0_{corr} - i^{inh}_{corr}}{i^0_{corr}}\right) \quad (1)$$

where $i^0_{corr}$ and $i^{inh}_{corr}$ are the uninhibited and inhibited corrosion current densities respectively, determined by extrapolation of Tafel lines. The measurement of the corrosion current and potential were very reproducible. Besides to the reproducibility of the corrosion current determination, the accuracy in the calculation, which was about 5%, was mainly associated with the reduced cathodic Tafel region. However, the general tendency of the organic compounds on the electrochemical response of copper was similar.

## Theoretical calculation details

### Energy and charge descriptors

Theoretical calculations were performed with the Gaussian98 package [28]. The geometries of benzotriazole and its derivatives (Fig. 1) were fully optimized at the Density Functional Theory level of calculation, with the exchange [29] and correlation functional B3LYP [30] and the 6-31G (d) basis set. Theoretical calculations were done in solution phase, using the PCM model [31–39] and water as the solvent. Two theoretical descriptors were separately considered, energy and charge. The bonding energy ($\Delta E$) was calculated as the difference between the total energies ($E_T$) of the fully protonated structure ($BTAH_2^+$) and the conjugate base (BTAH) and the proton:

$$\Delta E = E_T(BTAH_2^+) - (E_T(BTAH) + E_T(H^+)) \quad (2)$$

On the other hand, the charge analysis descriptor ($\Delta q_N$) was formulated as the difference between the charge at the nitrogen atoms of the fully protonated form $BTAH_2^+$ and of the partial protonated form BTAH. The last form was simulated by considering a large N–H distance of 50 Å for the nitrogen in position 2. We employed the Mulliken charge analysis for estimating the charge descriptor.

$$\Delta q_N = q_N(BTAH_2^+)_{\vec{r}(N\text{-}H)=\text{normal}} - q_N(BTAH_2^+)_{\rightarrow(N2-H)=50\,\text{Å}} \quad (3)$$

where $q_N(BTAH_2^+)_{\vec{r}(N\text{-}H)=\text{normal}}$ is the charge of the nitrogen atoms in the optimized protonated forms, with

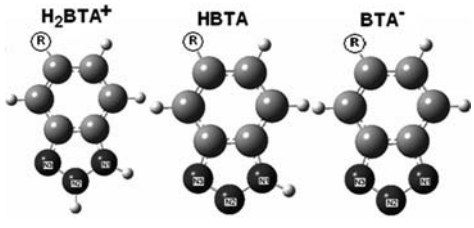


**Fig. 1** The molecular structure of the fully and partially protonated benzotriazole according to the work of Fagel et al. [47]. B3LYP/6-311G level theory

a normal N–H distance in the range of 1.04 and 1.09 Å, and $q_N(BTAH_2^+)_{\vec{r}(N2-H)=50\,Å}$ is the charge of the nitrogen atoms in the optimized form, with a N2–H distance of 50 Å. As previously mentioned, this last condition simulates the BTAH form.

### Condensed Fukui function

In order to investigate the preferred site of the BTAH molecule to interact with copper, the Fukui function of the three nitrogen atoms in this molecule was calculated. Parr and Yang [40] proposed the Fukui function $f(\vec{r})$, like a local reactivity index derived of the Density Function Theory. This function is an important descriptor to express the tendency of the electronic density to deform at a given position to accept or donate electrons.

$$f(\vec{r}) \equiv \left(\frac{\delta\mu}{\delta v(\vec{r})}\right)_N = \left(\frac{\partial\rho(\vec{r})}{\partial N}\right)_{V(\vec{r})} \quad (4)$$

where μ is the electronic chemical potential, $v(\vec{r})$ is the external potential, and N corresponds to the total number of electrons. The application of a frozen core approximation to $f(\vec{r})$ leads to the following definition:

$$f^+(\vec{r}) \approx \rho_{\mathrm{LUMO}}(\vec{r}) \quad (5)$$

$$f^-(\vec{r}) \approx \rho_{\mathrm{HOMO}}(\vec{r}) \quad (6)$$

$\rho_{\mathrm{LUMO}}$ and $\rho_{\mathrm{HOMO}}$ correspond to the electronic density of the LUMO and HOMO molecular orbitals, respectively. Equations 5 and 6 can also be condensed to atomic regions $k$ [41], leading to the following operational relation

$$f_k^+ \approx f_{k,}^+\mathrm{LUMO} = \rho_{k,}\mathrm{LUMO} = c_{ik,}^2\mathrm{LUMO} \quad (7)$$

$$f_k^- \approx f_{k,}^-\mathrm{HOMO} = \rho_{k,}\mathrm{HOMO} = c_{ik,}^2\mathrm{HOMO} \quad (8)$$

where $\rho_{k,\mathrm{LUMO}}$ and $\rho_{k,\ \mathrm{HOMO}}$ are the electronic density of the atom $k$ evaluated in LUMO and HOMO respectively. $C_{ik,\mathrm{LUMO}}$ and $C_{ik,\mathrm{HOMO}}$ are the eigenvectors of the atom $k$ in the given molecular orbitals, $f_k^+$ is used to analyze the reactive sites, where the electron receiving process occurs in the system (nucleophilic attack), $f_k^-$ is used to analyze the reactive sites where, one electron leaving process occurs in the system (electrophilic attack).

Equations 6 and 7 provide information about the reactive sites in the molecule. It is important to consider that the Fukui functions are only valid in evaluating soft–soft interactions between the two species. We used Fukui function to find the most probable active site of the benzotriazole molecule to interact with copper.

## Results and discussion

### Electrochemical measurements

#### *The open circuit potential*

In general, the open circuit potential (OCP) of copper (Fig. 2) shifted in the positive direction from the commencement of the test by about 30 mV, reaching a constant value of −0.503 V after 1,600 s. This is consistent with a $Cu/CuCl/CuCl_2^-$ system and with the *E*–pH equilibrium diagrams for the $Cu–Cl^–H_2O$ at different activities of chloride ions [12, 13]. A relatively similar OCP behaviour of copper is observed in the presence of low concentration of the additives, $10^{-5}$–$10^{-4}$ M, but the OCP values over the whole testing time are more negative than in the absence of the additive. In Fig. 2, the OCP values in the presence of $10^{-5}$ and $10^{-4}$ mol $l^{-1}$ of the additive are displaced by about 5 mV in the negative direction, with respect to that of copper in the inhibitor free solution. Such a negative displacement of the OCP augments with increasing the additive concentration to $10^{-3}$ mol $l^{-1}$, giving values dependent on the particular additive, about 25 mV for BTAH and 40 mV for 5-chloro and 5-methyl BTAH. In the case of $10^{-3}$ mol $l^{-1}$ of 5-methyl benzotriazole the OCP of copper shifted in the negative direction at the beginning of the experiment, but then moved rapidly along the opposite direction. At a high additive concentration of benzotriazole and 5-methyl benzotriazole, $10^{-2}$ M, the OCP of copper had a negative trend over the whole testing time, reaching a constant value of −0.63 and −0.62 V after 1,600 s. In contrast, the influence of 5-chloro benzotriazole at a concentration of $10^{-2}$ mol $l^{-1}$ causes a marked increase in the OCP of copper from the beginning of the rest to −0.38 V after 1,600 s. The different influences of the additive in the OCP of copper are discussed later with regard to the potentiodynamic experiments and theoretical calculations.

#### *Polarization curves*

Figures 3, 4 and 5 show typical polarization curves for copper in aerated 0.1 HCl in the absence and presence of different concentrations of benzotriazole and its derivatives. In each case the cathodic and anodic curves were recorded after the copper electrode had been exposed to the electrolyte for 30 min. In the inhibitor-free solution, oxygen reduction was observed in the cathodic region and copper dissolution in the anodic region. In the presence of $10^{-5}$ and $10^{-4}$ mol $l^{-1}$ of the additives, the potential–current responses are slightly different to those observed in their absence. In the cathodic run, a "hump" can be observed at low overpotentials, followed by the limited diffusion reduction of molecular oxygen. This has been associated to the presence of both adsorbed

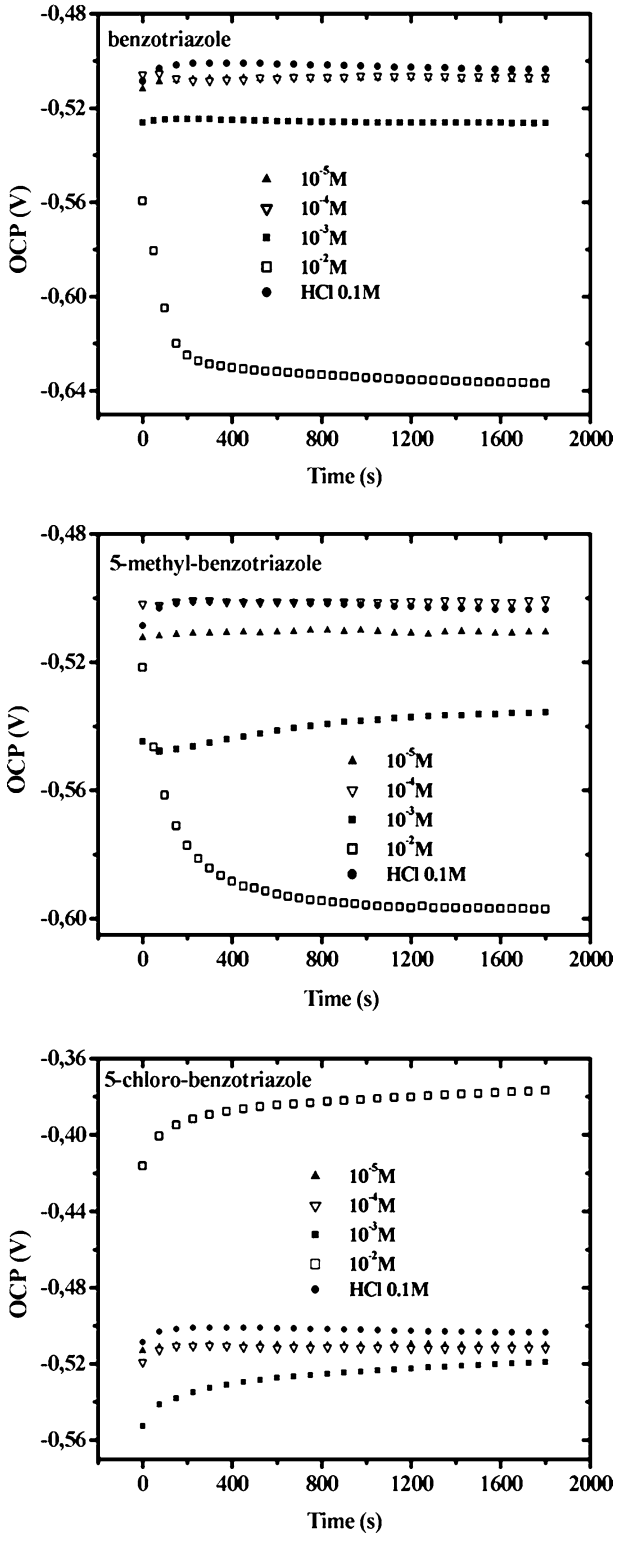


**Fig. 2** The variation of the open circuit potential (*OCP*) of copper with time, in the absence and presence of different concentrations of benzotriazole and its derivatives in 0.1 mol $l^{-1}$ HCl. The potentials are referred to the mercury/mercury sulfate electrode

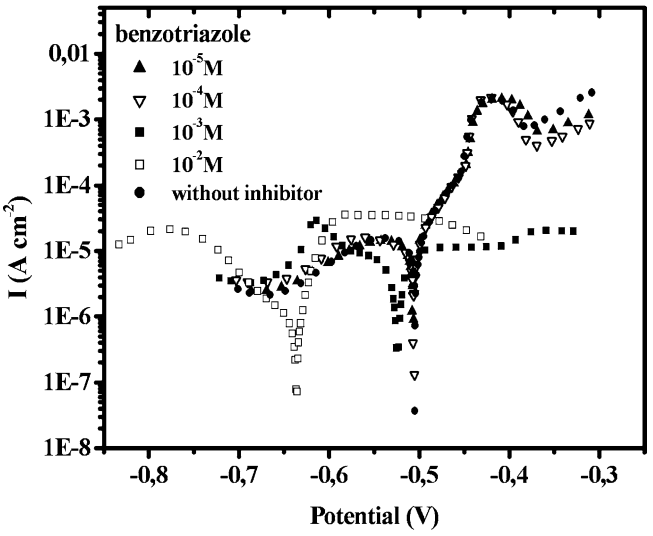


**Fig. 3** Polarization curves of copper in 0.1 mol $l^{-1}$ HCl, in the absence and presence of different concentrations of benzotriazole. The potentials are referred to the mercury/mercury sulfate electrode

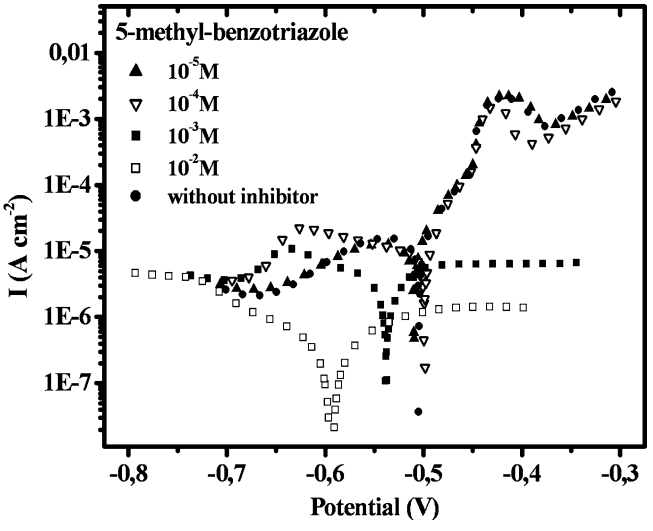


**Fig. 4** Polarization curves of copper in 0.1 mol $l^{-1}$ HCl, in the absence and presence of different concentrations of 5-methyl-benzotriazole. The potentials are referred to the mercury/mercury sulfate electrode

intermediates formed during $O_2$ reduction or adsorbed chloride ions [33, 42]. The hump tends to disappear with increasing the additive concentration and a second wave is revealed at higher overpotentials. A very steep rise in the inhibitive effect is observed when concentration goes from $10^{-4}$ mol $l^{-1}$ to $10^{-3}$ mol $l^{-1}$. For benzotriazole and 5-methyl benzotriazole the inhibitive effect comes together with a displacement of the corrosion potential in the negative direction. Such a displacement has been previously related to blocking of the cathodic sites, which in the case of copper in chloride solutions has been mainly associated with chloride-free copper regions. Adsorption of benzotriazole species, possibly$BTAH_2^+$, may hinder $O_2$ diffusion and the displacement of adsorption of the $O_2$ reduction intermediates [4, 44]. A

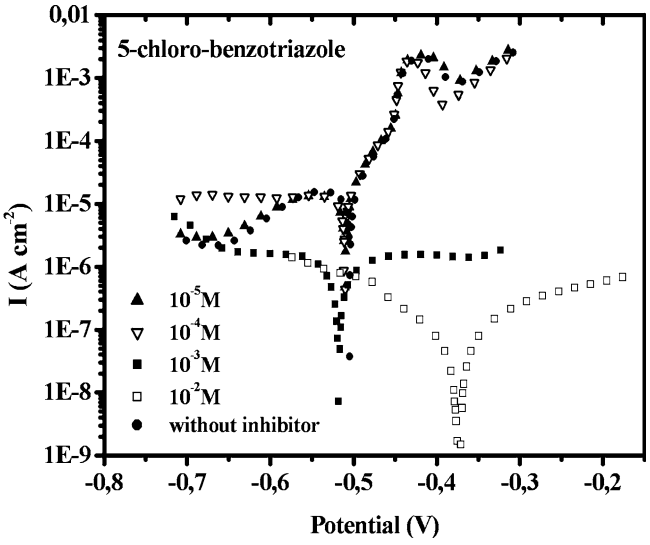


**Fig. 5** Polarization curves of copper in 0.1 mol $l^{-1}$ HCl, in the absence and presence of different concentrations of 5-chloro-benzotriazole. The potentials are referred to the mercury/mercury sulfate electrode

different situation is observed in the inhibitive influence of 5-chloro-benzotriazole, where corrosion inhibition proceeds without a change in the corrosion potential of copper. With increasing the inhibitor concentration to $10^{-2}$ mol $l^{-1}$, the BTAH and 5-methyl BTAH displace further the corrosion potential in the cathodic direction. In contrast, the 5-chloro benzotriazole shifts the corrosion potential in the anodic direction.

As observed in Table 1, the corrosion IE calculated from Eq. 1 augments with increasing the corrosion inhibitor concentration.

From comparison of the data in Table 1, the inhibiting efficiency of the BTAH derivatives, as a function of the concentration, increased more rapidly than that of BTAH. This accounts for the more negative OCP in the case of 5-methyl benzotriazole, which may be associated with a greater interaction of this additive on the cathodic sites of the copper electrode. On the other hand, the increased inhibiting efficiency of 5-chloro-benzotriazole with increasing concentration seems to be related to a change in the inhibition mechanism. Such a positive displacement in the corrosion potential of copper has been reported for benzotriazole in neutral solution, where the formation of a $Cu(BTA)_n$ oligomer is suggested to limit copper dissolution [3, 4, 8, 9, 13]. From Table 1, the influence of the 5-chloro benzotriazole in the corrosion potential of copper is concentration dependent, suggesting that the potential depends on the equilibrium constant of several reactions.

In general the information obtained from polarization curves agrees with the behaviour of the OCP of copper in the absence and presence of the additives. Thus, the corrosion potentials in Table 1 are relatively similar to the OCP values of copper in Fig. 2. Further, from Table 1 all the additives reduce the copper corrosion in 0.1 mol $l^{-1}$ HCl and the inhibiting efficiency follows the order: 5-chloro benzotriazole > 5-methyl benzotriazole > benzotriazole.

### *Adsorption of the additives*

From the graphic surface coverage (θ) versus concentration ($C$), which is not shown here, the adsorption of the three inhibitors follows a Langmuir isotherm. The surface coverage values (θ) were obtained from the following equation:

$$\theta = \frac{E}{100} \tag{9}$$

where $E$ corresponds to the corrosion inhibition efficiency taken from the data in Table 1. A plot of log [θ /(1− θ)] versus log $C$ was used to test for Langmuir behaviour, which is shown in Fig. 6. From the value of $K$, obtained from the ordinate intercept, the free energy of adsorption of the benzotriazoles on copper was calculated by the expression below:

$$K = A\exp\left(\frac{-\Delta G}{RT}\right) \tag{10}$$

**Table 1** Variation of the inhibition efficiency (IE), corrosion potential ($E_{corr}$), corrosion current density ($I_{corr}$), and the anodic and cathodic slopes ($b_a$ and $b_c$) in the absence and presence of different concentrations of benzotriazole and its derivatives

| Inhibitor | $C$ (mol $l^{-1}$) | $E_{corr}$ (V) | $I_{corr}$ (A $cm^{-2}$) | $b_a$ (mV/dec) | $b_c$ (mV/dec) | IE (%) |
|---|---|---|---|---|---|---|
| Benzotriazole | 0 | −0.511 | $8.5\times10^{-6}$ | 35 | 63 | 0.00 |
| | $10^{-5}$ | −0.508 | $8.6\times10^{-6}$ | 37 | 70 | 0.00 |
| | $10^{-4}$ | −0.504 | $7.0\times10^{-6}$ | 39 | 83.1 | 16.98 |
| | $10^{-3}$ | −0.525 | $3.8\times10^{-6}$ | 51 | 98 | 54.95 |
| | $10^{-2}$ | −0.638 | $7.8\times10^{-7}$ | 23 | 71 | 90.80 |
| 5-Methyl-benzotriazole | $10^{-5}$ | −0.511 | $7.8\times10^{-6}$ | 32 | 75 | 8.19 |
| | $10^{-4}$ | −0.499 | $5.7\times10^{-6}$ | 23 | 49 | 32.78 |
| | $10^{-3}$ | −0.536 | $1.5\times10^{-6}$ | 50 | 73 | 82.46 |
| | $10^{-2}$ | −0.599 | $1.8\times10^{-7}$ | 60 | 119 | 97.87 |
| 5-Chloro-benzotriazole | $10^{-5}$ | −0.512 | $6.7\times10^{-6}$ | 29 | 49 | 21.34 |
| | $10^{-4}$ | −0.510 | $7.3\times10^{-7}$ | 31 | 83 | 91.45 |
| | $10^{-3}$ | −0.510 | $4.9\times10^{-7}$ | 60 | 85 | 94.28 |
| | $10^{-2}$ | −0.397 | $2.7\times10^{-8}$ | 59 | 44 | 99.79 |

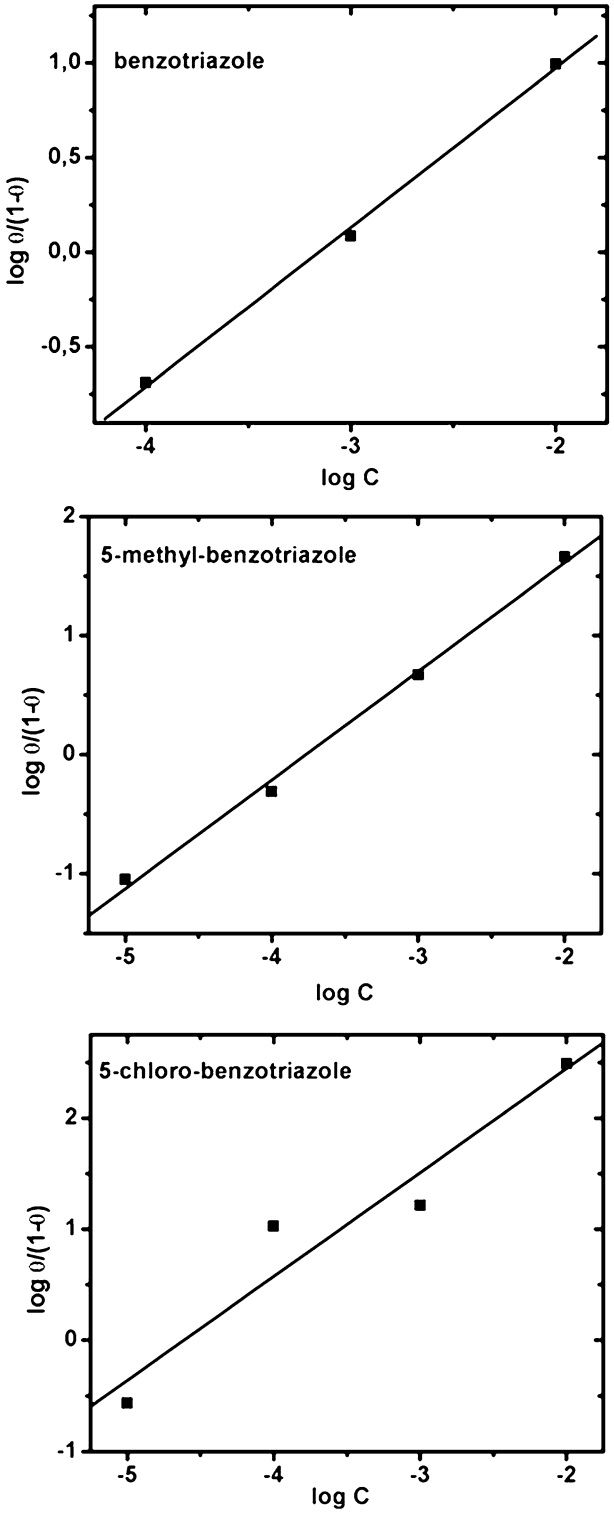


**Fig. 6** The surface coverage and concentration relationship for benzotriazole and its derivatives according to a Langmuir behaviour

where $A$ is a constant associated with 1/(solvent concentration), which in the case of aqueous solutions is about 1/55.5 $mol^{-1}$ $l^{-1}$, $\Delta G$ is the Gibbs free energy, $T$ is the absolute temperature (K) and $R$ is the gas constant.

The free energy of the adsorption of benzotriazole, 5-methyl benzotriazole and 5-chloro benzotriazole were −3.8, −4.7 and −5.9 kcal $mol^{-1}$, respectively. These rather low values indicate that physisorption of the additives on copper occur. This indicates that the additive, possibly$BTAH_2^+$ species, interacts weakly with the electrode surface and that, such an interaction increases with substituents in the position 5. The adsorption of the$BTAH_2^+$ and its derivatives with the metal surface should be competitive with the interactions of the ions in the solution. Very aggressive anions, such as chlorides, in the present experimental conditions, notably reduce the action of the additives at concentrations lower than $10^{-3}$ mol $l^{-1}$.

## IE–Hammett parameters relationship

In order to characterize the substituent effect, we used the Hammett parameter (σ).

The Hammett equation in the form:

$$\log\left(\frac{k}{k_0}\right) = \rho\sigma \tag{11}$$

or

$$\log\left(\frac{K}{K_0}\right) = \rho\sigma \tag{12}$$

is applied to the influence of *meta*- or *para*-substituents $X$ on the reactivity of the functional group $Y$ in the benzene derivative *m*- or *p*-XC6H4Y. $k$ or $K$ is the rate or equilibrium constant, respectively, for the given reaction of *m*- or *p*-XC6H4Y; $k_0$ or $K_0$ refers to the reaction of C6H5Y, where $X = H$; σ is the substituent constant characteristic of *m*- or *p*-*X*: ρ is the reaction constant characteristic of the given reaction of *Y*. The equation is often encountered in a form with log $k_0$ or log $K_0$ written as a separate term on the right hand side, e.g.

$$\log k = \rho\sigma + \log k_0 \tag{13}$$

or

$$\log K = \rho\sigma + \log K_0 \tag{14}$$

log $K_0$ is then the intercept corresponding to $X = H$ in a regression of log $k$ or log $K$ on σ. From the work of Hammett [45, 46], the physical meaning of σ is as follows: the negative σ values imply an electron-donor character of the substituent, while positive values imply an electron acceptor character.

Figure 7 shows the relationship between the corrosion potential, obtained for three additive concentrations, $10^{-4}$, $10^{-3}$ and $10^{-2}$ mol $l^{-1}$, and the Hammett parameter (σ). As observed at concentration of $10^{-4}$ mol $l^{-1}$ (Fig. 7a) the corrosion potential reveals a linear relationship with σ, of a positive slope. With increasing the additive concentration to $10^{-3}$ (Fig. 7b), the relationship between the corrosion potential is also

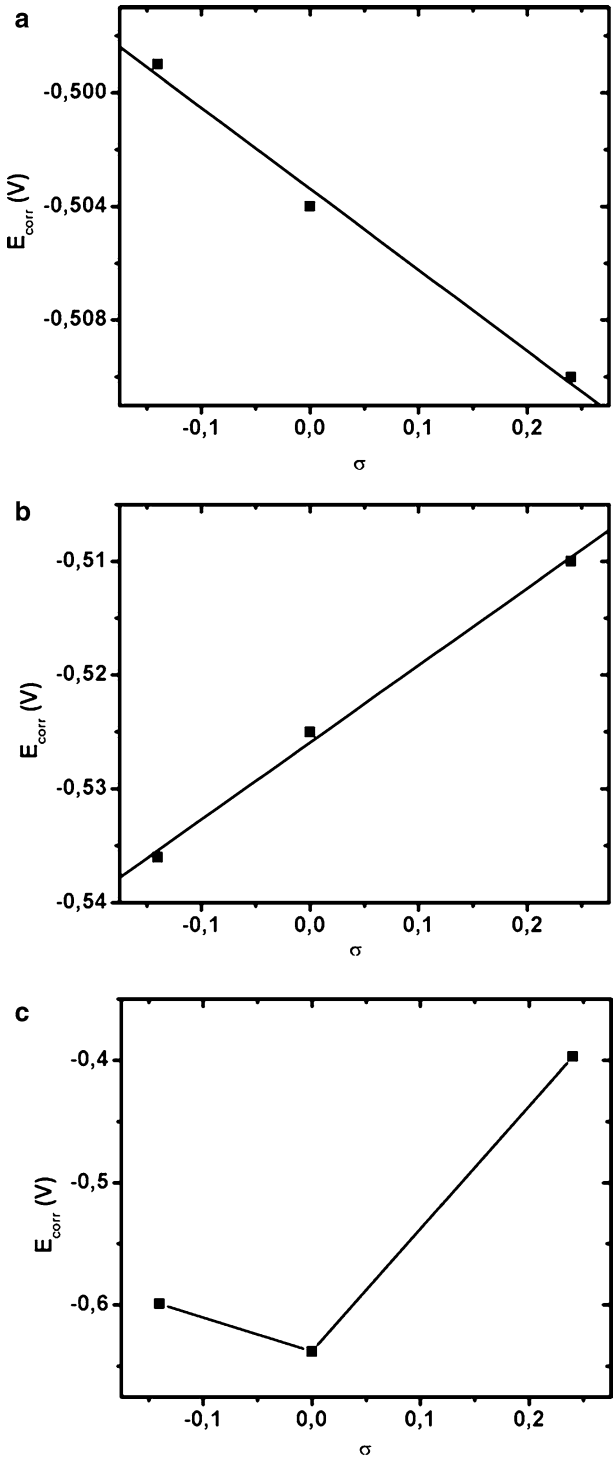


**Fig. 7** The corrosion potential and Hammett parameter relationship for different concentration of benzotriazole and its derivatives. **a** $10^{-4}$ mol $l^{-1}$; **b** $10^{-3}$ mol $l^{-1}$ and **c** $10^{-2}$ mol $l^{-1}$

linear, but with a negative slope. Further, for the higher concentration in Fig. 7c, the $E_{corr}/\sigma$ relationship changes to a concave down curve. It is interesting that when the corrosion inhibition efficiency is plotted against the Hammett parameter (Fig. 8), for all the additive concentrations a concave down curve is revealed. From the work of Schreck [46] a non-linear Hammett relationship is revealed when the mechanism of a reaction changes as a result of substituents or, when the measured rate constant is actually a composite quantity depending on the rate and equilibrium constant of several reactions steps.

Considering the influence of the different substituents on the inhibiting action of benzotriazole, particularly the $E_{corr}/\sigma$ relationship, we wanted to investigate the origin of such a behaviour. Taking into account the *E*–pH diagrams for the Cu–BTAH–$Cl^-$–$H_2O$ systems [13, 47], in solution containing 0.67 activity of [$Cl^-$] and in the presence of $10^{-4}$ total activity of dissolved BTAH species, the main benzotriazole species at pH 1 are $BTAH_2^+$ in equilibrium with BTAH. Therefore, the inhibitor specie inhibiting copper dissolution is mainly the fully protonated benzotriazole. For benzotriazole and 5-chloro benzotriazole, the adsorption of the fully protonated species shifts the corrosion potential of copper in the negative direction, revealing a cathodic behaviour. However, this is contrary to the influence of 5-chloro BTAH at concentrations higher than $10^{-2}$ mol $l^{-1}$. From the *E*–pH diagram the presence of $BTA^-$ is only possible at pH higher than three. Nevertheless, with increasing the additive to $10^{-2}$ total activity of dissolved BTAH species, the stable pH region of $BTA^-$ is enlarged and the presence of this specie is possible at pH about 1.5. In the case of benzotriazole and methyl-benzotriazole the enlargement of the pH region where BTA is stable does not affect the BTAH in solution, since the pK of the first proton is about 1 [12, 13]. Regarding the electron donor characteristic of the methyl group it is highly possible that the pK for the first proton in the 5-methyl benzotriazole is lower than that of the benzotriazole. Therefore, the main species for these two additives in solution, over the whole concentration range, are $BTAH_2^+$ and BTAH. Based on a early work of Fagel et al. [48], our hypothesis is that the electron-acceptor characteristic of chloro in position 5 of benzotriazole affects the acidity of the hydrogen atom in position 2. This allows the formation of the partially protonated species (BTAH) to an extent greater than that of the unsubstituted benzotriazole, which is represented in Eq. 15.

$$BTAH_2^+ \rightarrow BTAH + H^+ \quad k = 0.1 \tag{15}$$

The previous equilibrium is expected to influence differently the equilibriums in Eqs. 16 and 17, which are discussed later with regards to the theoretical results.

$$BTAH \leftrightarrow BTA^- + H^+ \quad k = 6.31 \times 10^{-9} \tag{16}$$

$$CuCl_2^- + BTAH \leftrightarrow Cu\text{-}BTA + H^+ + 2Cl^- \quad k = 1.54 \times 10^2 \tag{17}$$

From the previous analysis, the acidity constant for the equilibrium in Eq. 15 is critical. Considering this, we

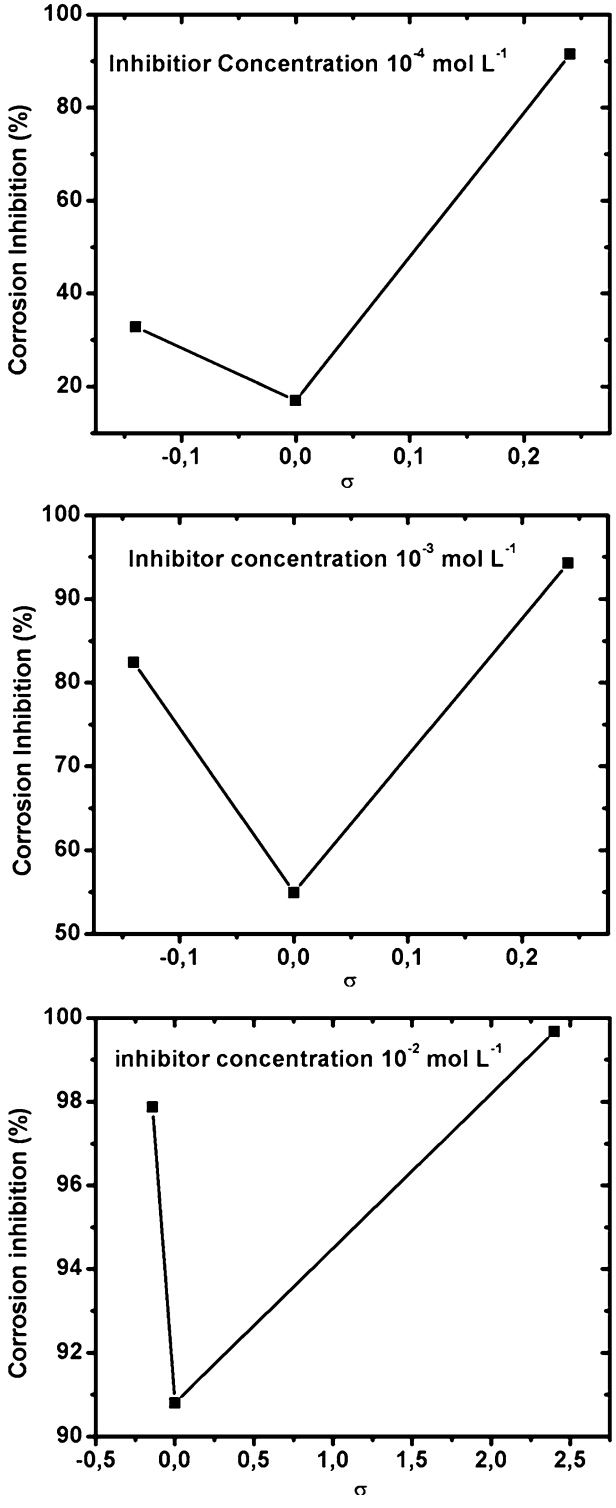


**Fig. 8** The efficiency of corrosion inhibition and Hammett parameter relationship for different concentration of benzotriazole and its derivatives

have carried out theoretical calculations to estimate if the presence of chloro affects the bonding energy of the hydrogen bonded to the nitrogen of the higher acidity in the benzotriazole molecule (N2 in Fig. 1).

## Theoretical calculations

Tables 2 and 3 list, respectively, the bonding energies and the charge analysis descriptor values for all the studied compounds. From Table 2, the bonding energies increase when the substituent in position 5 has a donor electronic characteristic and decrease when the substituent has an acceptor electronic characteristic. This suggests that the electronic density of substituent in position 5 is important in stabilizing the conjugate base after proton dissociation. Further, the lower bonding energy for the N2–H bond in 5-chloro benzotriazole predicts a higher acidity constant for the equilibrium in Eq. 11. From Table 3, the charge of the nitrogen atom (N2) after loosing the hydrogen atom increases when the chloro substituent is present in position 5. This implies that with the formation of BTAH, the nitrogen in position 2 (N2) will be the atomic region where the reaction between the organic molecule and copper will take place. The $f_k^+$ condensed Fukui indexes for $H_2BTA^+$, 5-$CH_3$-$H_2BTA^+$ and 5-Cl-$H_2BTA^+$ were also determined and are presented in Figs. 9–11. We focused our study only in $f_k^+$ because we are interested in identifying the sites deficient in electrons. In all the graphics can be observed that the highest value of $f_k^+$ is found in N2 atom (Fig. 1). Because a highest value of a condensed Fukui function represents a more reactive site upon to an electronic perturbation, we conclude that the N2 atom corresponds to the site with a highest probability to undergo a nucleophilic attack in the benzotriazole derivative. Then, beside to the higher acidity of 5-chloro benzotriazole, the nitrogen atom in position 2 would be the preferred interaction site with copper when loosing the hydrogen atom.

From the previous results the corrosion inhibition mechanism observed for 5-chloro benzotriazole at concentrations higher than $10^{-3}$ mol $l^{-1}$ is associated with the electron acceptor characteristics of the chloro group and the dependence of equilibria in Eqs. 15–17 on the concentration of species in solution. From Table 2, the presence of chloro in position 5 of the organic molecule reduces the bonding energy of the hydrogen by a factor of two in the nitrogen atom in position 2. This predicts an increase in the acidity of the first proton in the benzotriazole molecule (N2 in Fig. 1) and a displacement of the equilibrium in Eq. 15 to the BTAH form. From Table 1, however, such a concentration increase at the electrochemical interface does not affect the corrosion potential of copper for an inhibitor concentration up to $10^{-3}$ mol $l^{-1}$ (Table 1); with corrosion inhibition proceeding mainly by a mixed mechanism. When the additive concentration changes to $10^{-2}$ mol $l^{-1}$, further corrosion inhibition comes together with a displacement of the corrosion potential of copper in the positive direction, suggesting a passivation process is occurring and associated to the formation of CuBTA [1–8]. Taking into consideration the *E*–pH diagram for the Cu–BTAH–$Cl^-$–$H_2O$ [13] and the low value of the acidity constant in Eq.16, it is unlikely that the source of $BTA^-$

**Table 2** The bonding energy descriptor ($\Delta E$) for $H_2$-BTA$^+$, 5-$CH_3$-$H_2$BTA$^+$ and 5-Cl-$H_2$BTA$^+$ . $E_H^+ = -0.415472$ Hartrees

| Substituent in position 5 | $E$ (Hartrees) 5-X-$H_2$BTA (acid) | $E$ (Hartrees) 5-X-HBTA (conjugated based) | $\Delta E$ (Hartrees) | $\Delta E$ (kcal) |
|---|---|---|---|---|
| –H | −396.2086299 | −395.7661744 | −0.0269835 | −16.93 |
| –$CH_3$ | −435.5169452 | −435.0723292 | −0.029144 | −18.29 |
| –Cl | −855.7694232 | −855.3383789 | −0.0155723 | −9.77 |

**Table 3** The charge analysis descriptor ($\Delta q_N$) for $H_2$-BTA$^+$, 5-$CH_3$-$H_2$BTA$^+$ and 5-Cl-$H_2$BTA$^+$

| Substituent in position 5 | | $q_N$(net charge) 5-X-$H_2$BTA r(N-H) = normal | $q_N$ (net charge) 5-X-$H_2$BTA r(N2-H) = 50 Å | $\Delta q_N$ |
|---|---|---|---|---|
| –H | N1 | −0.53 | −0.31 | −0.22 |
| | N2 | −0.16 | −0.06 | −0.10 |
| | N3 | −0.21 | −0.13 | −0.08 |
| –$CH_3$ | N1 | −0.53 | −0.36 | −0.17 |
| | N2 | −0.17 | −0.02 | −0.15 |
| | N3 | −0.22 | −0.16 | −0.06 |
| –Cl | N1 | −0.51 | −0.39 | −0.12 |
| | N2 | −0.15 | 0.02 | −0.17 |
| | N3 | −0.19 | −0.17 | −0.02 |

species is derived from the equilibrium in Eq. 16. Considering this, an increase of the BTAH form is though to influence preferentially the equilibrium in Eq. 17, which described the reaction between the unsubstituted benzotriazole and the $CuCl_2^-$ complex [12, 13]. The electron charge transfer reaction involving the formation of the complex (Eq. 18) occurs rapidly to allow the copper surface to be in quasi equilibrium with the applied electrode potential [12, 13, 40]

$$Cu + 2Cl^- \rightarrow CuCl_2^- + e^- \quad (18)$$

With respect to the equilibrium in Eq. 17, it has been suggested that the required condition for the formation of a passivating layer of Cu–BTA is a concentration of BTAH in the bulk of the solution, which is greater than that of $CuCl_2^-$ at the outer Helmhotz plane [48]. The previous condition is determined by the equilibrium in Eq. 15, where the concentration of BTAH in the solution bulk depends on the acidity constant of benzotriazole and on the concentration of the additive. From this analysis, the higher acidity constant of 5-chlorobenzotriazole, with respect to that of the unsubstituted benzotriazole, predicts an increase of the 5-chloro BTAH concentration in the solution bulk and therefore, a displacement of the equilibrium in Eq. 13 to the right. The initial concentration of $CuCl_2^-$ is probably below $10^{-6}$ mol $l^{-1}$ [47], however, this is expected to increase with the resting time before the anodic polarization is

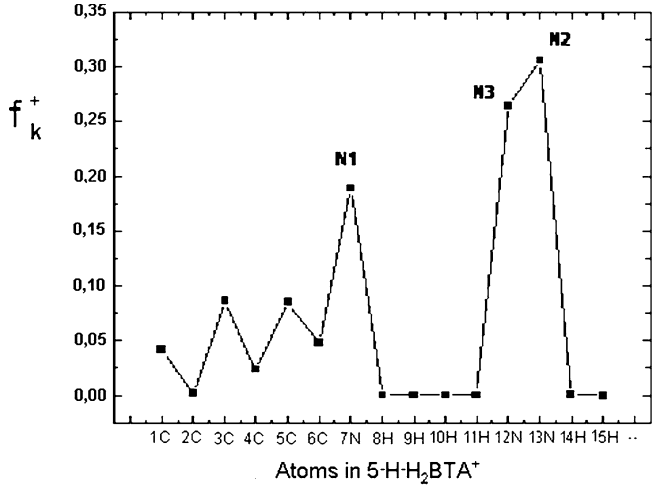


**Fig. 9** $f_k^+$ condensed Fukui indexes for 2H-benzotriazole calculated by the frozen core approximation. N1, N2 and N3, correspond to those included in Fig. 1

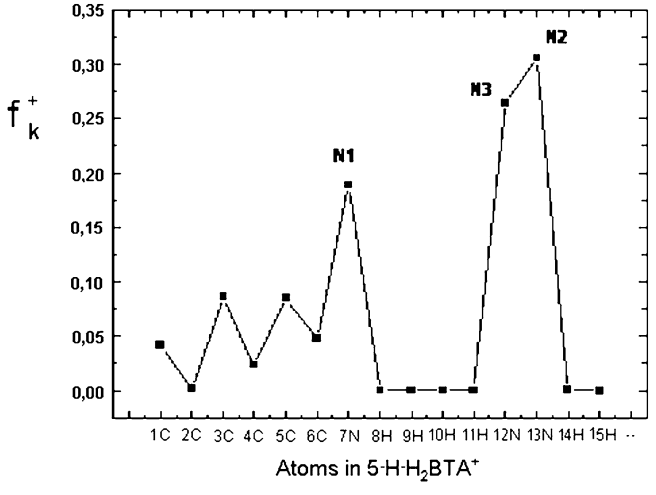


**Fig. 10** $f_k^+$ condensed Fukui indexes for 5-$CH_3$-2H-benzotriazole calculated by the frozen core approximation. N1, N2 and N3 correspond to those included in Fig. 1

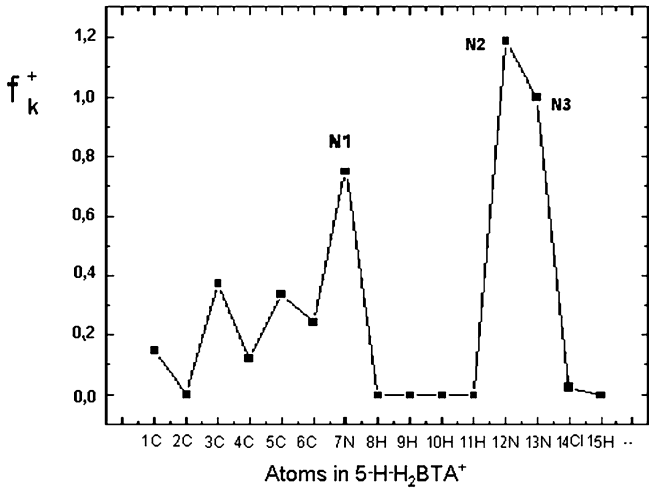


**Fig. 11** $f_k^+$ condensed Fukui indexes for 5-Cl-2H-benzotriazole calculated by the frozen core approximation. N1, N2 and N3 correspond to those included in Fig. 1

applied and with increasing the potential [13]. Further, the slow scan rate, 0.1 mV $s^{-}$, allows precipitation of CuBTA to be detected [13, 49].

In the case of benzotriazole and 5-methyl benzotriazole, the main species to interact with copper is the fully protonated, $BTAH_2^+$. The inability of benzotriazole to form Cu–BTA at low pH, even for a total activity of $10^{-2}$, has been extensively discussed by Desmond and Tromans [12, 13]. From Table 2, the electron-donor characteristic of the methyl group reduces further the possibility of benzotriazole to form Cu–BTA, which is reflected as an increase of the bonding energies of the hydrogen atom to N2 (Table 2). Therefore, the inhibiting action of benzotriazole and 5-methyl benzotriazole on copper corrosion is mainly associated with the physisorption of the fully protonated forms $BTAH_2^+$ on the copper surface.

## Conclusions

1. Benzotriazole and its derivatives inhibit copper corrosion in acid medium and the inhibition efficiency is dependent on the additive concentration, the greater the additive concentration, the higher the corrosion inhibition.
2. The organic compounds are physisorpted on the metal surface, following a Langmuir behaviour, with adsorption free energies between 3.9 kcal $mol^{-1}$ and 5.9 kcal $mol^{-1}$.
3. In the concentration range $10^{-5}$–$10^{-3}$ mol $l^{-1}$ all the additives follow a cathodic type behaviour, displacing the corrosion potential of copper in the negative direction.
4. At a concentration of $10^{-2}$ mol $l^{-1}$ a substituent effect on the corrosion IE appears, and a change from cathodic to anodic inhibition is revealed. From theoretical calculations, this is associated with the electron acceptor characteristic of chloro, increasing the acidity of benzotriazole and facilitating the formation of CuBTA.

**Acknowledgements** The authors are grateful to FONDECYT Líneas Complementarias (grant No. 8010006) for financial support.

## References

1. Dugdale I, Cotton JB (1963) Corros Sci 3:69
2. Cotton JB, Scholes IR (1967) Br Corros J 2:1
3. Poling GW (1970) Corros Sci 10:359
4. Mansfeld F, Smith T (1973) Corrosion 29:105
5. Youda R, Nishirahara H, Aramaki K (1990) Electrochim Acta 35:1011
6. Youda R, Nishirahara H, Aramaki K (1988) Corros Sci 28:87
7. Oggle ICG, Poling GW (1975) Can Metall Q 14:37
8. Fox PG, Lewis G, Boden PG (1979) Corros Sci 19:457
9. Chadwick C, Hashemi T (1978) Corros Sci 18:39
10. Bo-Shung Fang, Olson CG, Lynch DW (1986) Surf Sci 176:476
11. Hashemi T, Hogart CA (1988) Electrochim Acta 33:1123
12. Tromans D, Sun Ru-hong (1991) J Electrochem Soc 138:3235
13. Tromans D (1998) J Electrochem Soc 145:L42
14. Wu JS, Nobe K (1981) Corrosion 37:223
15. Tommesani L, Brunoro G, Frignani A, Monticelli C, Dal Colle M (1997) Corros Sci 39:1221
16. Frignani A, Fonsati M, Monticelli C, Brunoro G (1999) Corros Sci 41:1205
17. Frignani A, Fonsati M, Monticelli C, Brunoro G (1999) Corros Sci 41:1217
18. Hollander O, May R (1985) Corrosion 41:39
19. Tornkvist C, Thierry D, Bergman J, Liedberg B, Leygraf C (1989) J Electrochem Soc 136:58
20. Otieno-Alego V, Bottle SE, Schweinsberg DP (1996) In: Proceeding 13th international corrosion conference, Melbourne, Australia, 25–29 Nov 1996, 3:320
21. Ajmal M, Mideen AS, Quaraishi MA (1994) Corros Sci 36:79
22. Rosenfeld IL (1981) Corrosion inhibitors. McGraw-Hill, New York
23. Vosta J, Eliasek J (1971) Corros Sci 11:223
24. Chakrabarti A (1984) J Br Corros 19:124
25. Costa JP, Lluch JM (1984) Corros Sci 24:929
26. Xiao-Ci Y, Hong Z, Ming-Dao L, Hong-Xuang R, Lu-An Y (2000) Corros Sci 42:645
27. Khalil N (2003) Electrochim Acta 48:2635
28. Frisch MJ, Trucks GW, Schlegel HB, Scuseria GE, Robb MA, Cheeseman JR, Zakrzewski VG, Montgomery JA, Stratmann RE Jr, Burant JC, Dapprich S, Millam JM, Daniels AD, Kudin KN, Strain MC, Farkas O, Tomasi J, Barone V, Cossi M, Cammi R, Mennucci B, Pomelli C, Adamo C, Clifford S, Ochterski J, Petersson GA, Ayala PY, Cui Q, Morokuma K, Malick DK, Rabuck AD, Raghavachari K, Foresman JB, Cioslowski J, Ortiz JV, Baboul AG, Stefanov BB, Liu G, Liashenko A, Piskorz P, Komaromi I, Gomperts R, Martin RL, Fox DJ, Keith T, Al-Laham MA, Peng CY, Nanayakkara A, Challacombe M, Gill PMW, Johnson B, Chen W, Wong MW, Andres JL, Gonzalez C, Head-Gordon M, Replogle ES, Pople JA (1998) Gaussian 98, revision A9. Gaussian, Pittsburgh
29. Becke AD (1993) J Chem Phys 98:5648
30. Lee C, Yang W, Parr RG (1998) Phys Rev B 37:785
31. Cimiraglia R, Persico M, Tomasi J (1980) Chem Phys Lett 76:169
32. Miertus S, Scrocco E, Tomasi J (1981) Chem Phys 55:117
33. Miertus S, Tomasi J (1982) Chem Phys 65:239
34. Cossi M, Barone V, Cammi R, Tomasi J (1996) Chem Phys Lett 255:327
35. Cancès MT, Mennucci B, Tomasi J (1997) J Chem Phys 107:3032

36. Barone V, Cossi M, Tomasi J (1997) J Chem Phys 107:3210
37. Cossi M, Barone V, Mennucci B, Tomasi J (1998) Chem Phys Lett 286:253
38. Mennucci B, Tomasi J (1997) J Chem Phys 106:5151
39. Mennucci B, Cancès E, Tomasi J (1997) J Phys Chem B 101:10506
40. Parr R, Yang W (1984) J Am Chem Soc 106:4049
41. Yang W, Mortier W (1986) J Am Chem Soc 108:5708
42. Ghandehari MH, Andersen TN, Eyring H (1976) Corros Sci 16:123
43. Balakrishnan K, Venkatesan VK (1979) Electrochim Acta 24:131
44. Mansfeld F, Smith T, Parry EP (1971) Corrosion 27:289
45. Hansch C, Leo A, Taft RW (1991) Chem Rev 91:165
46. Schereck JO (1971) J Chem Educ 48:103
47. Pourbaix M (1995) Lectures on electrochemical corrosion, 3rd edn. NACE, Houston
48. Fagel JE, Galen WE (1951) J Am Chem Soc 73:4360
49. Tromans D, Li G (2002) J Electrochem Soc 5:B5